Predicting Drum Vibrations Using the Polar Wave Equation

Alexander Brimhall*, Zane Perry*, Luke Sellmayer*
alexander.brimhall@colorado.edu, zane.perry@colorado.edu,
luke.sellmayer@colorado.edu

12/11/2023

*University of Colorado, Boulder. Applied Math Department

1 Abstract

This project analyzes the motion of a drum head after being struck, using the two dimensional wave equation in polar form. The analysis focuses on the modes of vibration, as well as extending the basic wave equation to account for damping conditions that better model the real world. Differences in behavior are discussed when different locations of the drum are struck

2 Introduction

Despite the relative frequency with which wave-like phenomena occur in the real world, modelling this type of behavior is very complex and unattainable without making large assumptions and relying on numerical estimation. The two dimensional wave equation, given by

$$\frac{\partial^2 u}{\partial t^2} = c^2 \frac{\partial^2 u}{\partial x^2} \tag{1}$$

is only able to represent the most basic physical situations, in which boundary conditions are homogeneous and the only influence on the motion of particles is the initial conditions, not any external forces such as gravity or friction. This equation can be extended to multiple dimensions in order to analyze more interesting geometries, though complicated domains often further restrict what results can truly be extracted.

For this reason, drums allow for a very interesting analysis on their motion and behavior. They are widely seen throughout the real world, and yet the circular geometry of their boundaries lead to complex relationships and understandings of wave-like behavior. Even further, the above wave equation can be extended to account for damping terms that lead to even more accurate models of phenomena in the real world.

Drums also provide an interesting opportunity to distinguish between cases of radial symmetry, independent of the angular location, in comparison to the less restrictive case where wave propagation is uneven across the surface of the drum. These results lead to an interesting conclusion as to why many drum players know to avoid striking their drums directly in the center of the head, and instead to aim for unsymmetrical geometries.

3 Project Development

3.1 The Undamped Two Dimensional Wave Equation

3.1.1 Derivation

The equilibrium position for a drum lies in the x, y plane, meaning that $z = 0$. Our goal is to derive an equation that models the displacement of the drum in the z direction. We can first zoom in on a small portion of the drum head with side lengths Δx and Δy. The mass of this segment of the drum is then given by $m = \sigma(x, y)\Delta x\Delta y$ where $\sigma(x, y)$ is the density per unit area. For our purposes, we can assume that the density of the drum head is constant and does not vary in space. The main force acting on the drum is the tension from being clamped down on the frame, and therefore each individual segment of the drum is being pulled taut by the neighboring segments (we can assume these forces far outweigh any other influences such as gravity or friction). We can now model this using Newton's law of motion,

$$F = ma = \sigma\Delta x\Delta y\frac{\partial^2 z}{\partial t^2},$$

where F is the sum of all of the vertical tension forces. These tension forces in the y dimension are shown below in figure 1, where T is the tension of the drum. The sum of these forces in the vertical direction is then given by

$$\begin{aligned} F &= T\Delta y(z'(x + \Delta x) - z'(x)) \\ &= T\Delta y\Delta x\frac{(z'(x + \Delta x) - z'(x)}{\Delta x} \\ &\approx T\Delta x\Delta y\frac{\partial^2 z}{\partial x^2}. \end{aligned}$$

This can be done in the x direction as well to find the total force acting on the drum head segment. Plugging this in to the equation above then gives

$$\sigma\Delta x\Delta y\frac{\partial^2 z}{\partial t^2} = T\Delta x\Delta y\left(\frac{\partial^2 z}{\partial x^2} + \frac{\partial^2 z}{\partial y^2}\right)$$

$$\frac{\partial^2 z}{\partial t^2} = \frac{T}{\sigma}\nabla^2 z(x, y, t),$$

resulting in the 2 dimensional form of the wave equation.

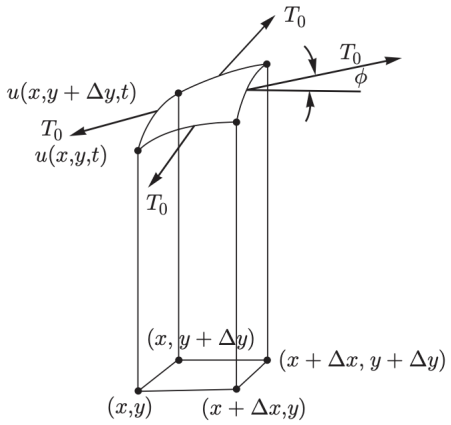

Figure 1: Approximation of a small segment of the drum head with tension forces acting on all sides[1]

3.1.2 Conversion to Polar Coordinates

A drum head can be modeled as a membrane on a disk $D = \{(x, y) : x^2 + y^2 < R^2\}$ with radius R. The membrane is attached to a frame, which is a circle $\partial D = \{(x, y) : x^2 + y^2 = R^2\}$ also of radius R. The height of the drum head, above or below its equilibrium position $z = 0$ at any given point (x, y) and time t is then the function $z(x, y, t)$.

As previously demonstrated, vibrations travelling through the drum head D can be modeled using the 2D wave equation

$$\frac{\partial^2 z}{\partial t^2} = c^2 \nabla^2 z(x, y, t), \tag{2}$$

where $c = \sqrt{\frac{T}{\sigma}}$, the speed of the wave. The boundary condition is $z(x, y, t) = 0$ on ∂D, since the membrane is fixed to the frame.

The circular symmetry of the drum head implies the use of polar coordinates, $z(r, \theta, t)$; D and ∂D can now be described as $D = \{(r, \theta) : 0 \leq r < R, 0 \leq \theta \leq 2\pi$, $\partial D = \{(r, \theta) : r = R, 0 \leq \theta \leq 2\pi$. Applying the Laplacian operator to these polar coordinates yields

$$\frac{\partial^2 z}{\partial t^2} = c^2 \left(\frac{1}{r} \frac{\partial}{\partial r} \left[r \frac{\partial z}{\partial r} \right] + \frac{1}{r^2} \frac{\partial^2 z}{\partial \theta^2} \right), \tag{3}$$

again with the boundary condition $z(R, \theta, t) = 0$. We will also impose two additional boundary conditions: that the solution is bounded at the origin, $|z(0, \theta, t)| < \infty$, and that the solution is periodic in θ, $z(r, -\pi, t) = z(r, \pi, t)$, $\frac{\partial z}{\partial \theta}(r, -\pi, t) = \frac{\partial z}{\partial \theta}(r, \pi, t)$.

3.1.3 Separation of Variables

To solve (2), we use separation of variables by letting $z(r,\theta,t) = F(r)G(\theta)H(t)$. Substituting into (2) and separating the time variable leads to

$$\frac{1}{c^2 H(t)}\frac{d^2H}{dt^2} = \frac{1}{r}\frac{1}{F(r)}\frac{d}{dr}\left[r\frac{dF}{dr}\right] + \frac{1}{r^2}\frac{1}{G(\theta)}\frac{d^2G}{d\theta^2} \tag{4}$$

Since the left side of the equation only depends on t while the right side only depends on r and θ, each side must equal a constant; assuming periodic solutions in time, we will choose the constant to be $-\lambda$, with $\lambda > 0$ This yields two equations:

$$\frac{d^2H}{dt^2} = -\lambda c^2 H(t) \tag{5}$$

$$\frac{1}{r}\frac{1}{F(r)}\frac{d}{dr}\left[r\frac{dF}{dr}\right] + \frac{1}{r^2}\frac{1}{G(\theta)}\frac{d^2G}{d\theta^2} = -\lambda \tag{6}$$

The r and θ variables can be further separated in (4):

$$-\frac{1}{G(\theta)}\frac{d^2G}{d\theta^2} = r\frac{1}{F(r)}\frac{d}{dr}\left[r\frac{df}{dr}\right]\frac{dF}{dr} + \lambda r^2 \tag{7}$$

Here, the left side of the equation only depends on θ while the right side only depends on r, so both must equal a constant: this time we will choose the constant to be μ assuming periodic solutions in θ, with $\mu \geq 0$. This yields two more equations:

$$\frac{d^2G}{d\theta^2} = -\mu G(\theta) \tag{8}$$

$$r\frac{d}{dr}\left[r\frac{dF}{dr}\right] + \left(\lambda r^2 - \mu\right)F(r) = 0 \tag{9}$$

The general solution to (7) is given by

$$G_m(\theta) = \begin{cases} c_1 \cos\left(\sqrt{\mu_m}\theta\right) \\ c_2 \sin\left(\sqrt{\mu_m}\theta\right) \end{cases}, \tag{10}$$

and the periodic boundary conditions imply that $\mu_m = m^2$ for $m = 0, 1, ...,$ giving an infinite family of solutions for $G_m(\theta)$, parameterized by m, up to some multiplicative constants.

3.1.4 Bessel Functions

Substituting $\mu_m = m^2$ into (8) and dividing by r yields

$$\frac{d}{dr}\left[r\frac{dF}{dr}\right] + \left(\lambda r - \frac{m^2}{r}\right)F(r) = 0 \tag{11}$$

Using the substitution $u = \sqrt{\lambda}r$ transforms (10) into Bessel's differential equation

$$u^2 \frac{d^2F}{du^2} + u\frac{dF}{du} + \left(u^2 - m^2\right) F(r) = 0 \tag{12}$$

which has the Bessel equations as its solution,

$$F_m(r) = \begin{cases} c_3 J_m\left(\sqrt{\lambda r}\right) \\ c_4 Y_m\left(\sqrt{\lambda r}\right) \end{cases} \tag{13}$$

However $Y_m\left(\sqrt{\lambda}r\right)$ is asymptotically unbounded at $r = 0$ and so does not satisfy the boundary condition $|z(0, \theta, t)| < \infty$; this allows us to eliminate it from the solution. The boundary condition $z(R, \theta, t) = 0$ implies that $\lambda_{m,n} = \left(\frac{Z_{mn}}{R}\right)^2$, where u_{mn} is the nth zero ($n = 1, 2, ...$) of $J_m(u)$, leading to the infinite family of solutions (up to a multiplicative constant),

$$c_3 F_{m,n}(r) = J_m\left(\sqrt{\lambda_{m,n}}r\right), \tag{14}$$

and we see that F is now parameterized by m and n. Finally, using the calculated value for $\lambda_{m,n}$ (which are all positive), the solution to (4) is given by

$$H_{m,n}(t) = \begin{cases} c_5 \cos\left(c\sqrt{\lambda_{mn}}t\right) \\ c_6 \sin\left(c\sqrt{\lambda_{mn}}t\right) \end{cases}, \tag{15}$$

again parameterized by m and n and differing up to a multiplicative constant.

3.1.5 Modes of Vibration

Combining (9), (13), and (14) yields the solution for the individual modes

$$z_{m,n}(r, \theta, t) = c_3 J_m\left(\sqrt{\lambda_{m,n}}r\right) \cdot \begin{cases} c_1 \cos\left(\sqrt{\mu_m}\theta\right) \\ c_2 \sin\left(\sqrt{\mu_m}\theta\right) \end{cases} \cdot \begin{cases} c_5 \cos\left(c\sqrt{\lambda_{mn}}t\right) \\ c_6 \sin\left(c\sqrt{\lambda_{mn}}t\right) \end{cases}. \tag{16}$$

The individual modes are characterized by the tuple (m, n); m refers to the number of nodal lines that span the diameter of the membrane, known as nodal diameters, while n refers to the number of nodal circles that wrap the circumference of the drum. [3]. A "node" refers to a place on the membrane where oscillations don't occur. The angular frequency of a given (m, n) node is given by $\omega_{m,n} = c\sqrt{\lambda_{m,n}}$, meaning its frequency is given by $f_{m,n} = \frac{\omega_{m,n}}{2\pi}$. An important consequence of this is since c is determined by the tension and density of the drum, the note that a drum plays is dependent only on the material of the drum head and the tension of the drum skin; this is why increasing the tension of the drum results in a higher note being played.

The *fundamental mode*, $(0,1)$, shown in Figure 2, contains no nodal diameters and only one nodal circle, which is found where the membrane of the drum meets the frame; it also has the lowest frequency of all possible modes, $f_{0,1} = \frac{\omega_{0,1}}{2\pi}$. Continuing up the nodes by their frequency, the next two modes are the $(1,1)$ mode and the $(2,1)$ mode, shown in Figures 3 and 4 respectively; these have frequencies of $f_{1,1} \approx 1.593 \cdot f_{0,1}$ and $f_{2,1} \approx 2.135 \cdot f_{0,1}$. There are a countably infinite number of frequencies corresponding to all possible combinations of m and n for $m = 0, 1, ...$ and $n = 1, 2, ...$

Mathematica was used to create these figures by computing $z_{m,n}(r, \theta, t)$ for $0 \leq r < R$ and $0 \leq \theta \leq 2\pi$, for specific values of t. The values of t were chosen to include each mode's peak, trough, and equilibrium position, achieved by determining the period of the each mode, $T_{m,n} = 1/f_{m,n}$.

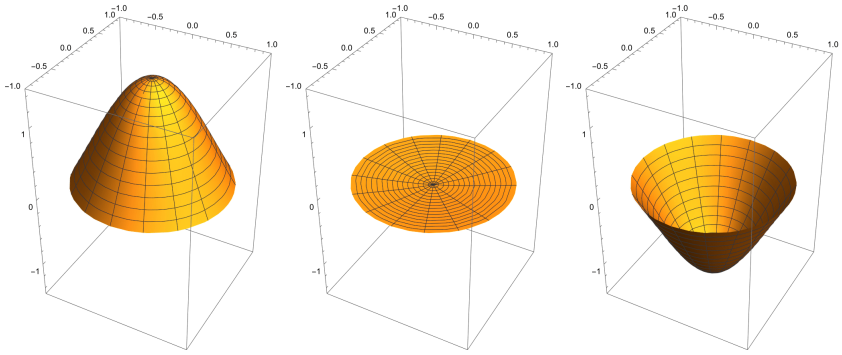

Figure 2: The fundamental mode

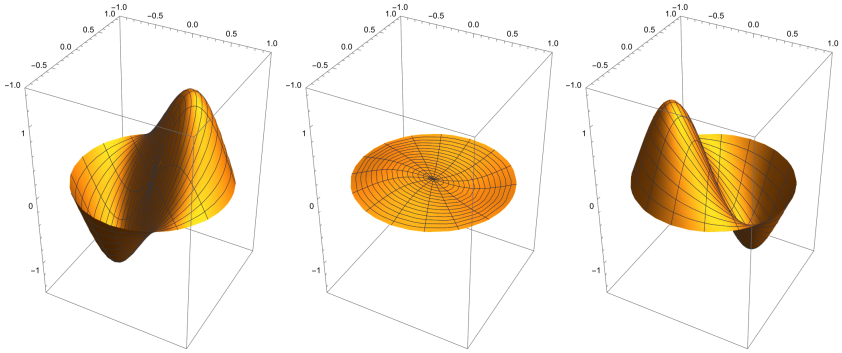

Figure 3: Mode (1, 1)

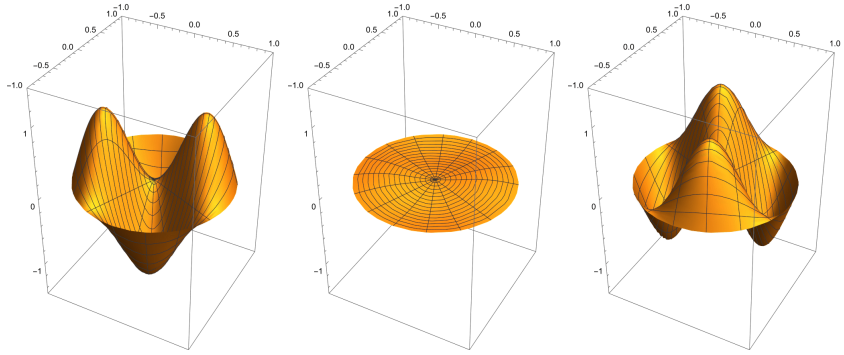

Figure 4: Mode (2, 1)

3.1.6 Initial Conditions

The striking of the drum with a drumstick can be modeled using an initial velocity distribution, $f(r, \theta)$, that represents the impulse provided to the drum. As the drum stick has not yet displaced the head of the drum, the initial position is at equilibrium[2]. This yields the following initial conditions:

$$z(r, \theta, 0) = 0 \tag{17}$$

$$\frac{\partial z}{\partial t}(r, \theta, 0) = f(r, \theta) \tag{18}$$

3.1.7 Solutions

We can first model the case where the drum head is struck in the exact center of the disc. This means that (16) and (17) are independent of theta; $z(r, 0) = 0$ and $\frac{\partial z}{\partial t}(r, 0) = f(r)$. The final solution will then also be independent of theta, corresponding to only containing modes where $m = 0$. This gives the following solution using superposition:

$$z(r, \theta, t) = \sum_{n=1}^{\infty} A_n J_0(\frac{u_{0,n}}{R} r) \sin\left(c\sqrt{\lambda_{0,n}} t\right) \tag{19}$$

$$A_n = \frac{1}{c\sqrt{\lambda_{0,n}}} \frac{\int_0^R f(r) J_0(\frac{u_n}{R} r) r dr}{\int_0^R [J_0(\frac{u_n}{R} r)]^2 r dr} \tag{20}$$

Where A_n is determined using the orthogonality principle of eigenfunctions. Note that the initial displacement condition resulted in the elimination of the cosine term in time.

If we were to instead strike the drum head anywhere else not in the center of the drum, we would no longer be able to assume angular independence; all possible modes, including modes where $m \neq 0$. The solution would instead be given by

$$z(r,\theta,t) = \sum_{m=0}^{\infty}\sum_{n=1}^{\infty} J_m(\frac{u_{m,n}}{R}r)\sin\left(c\sqrt{\lambda_{m,n}}t\right)\left(A_{n,m}\cos(m\theta) + B_{m,n}\sin(m\theta)\right) \tag{21}$$

$$A_{m,n} = \frac{1}{c\sqrt{\lambda_{m,n}}}\frac{\int_0^{2\pi}\int_0^R f(r)J_0(\frac{u_{m,n}}{R}r)\cos(m\theta)rdrd\theta}{\int_0^{2\pi}\int_0^R[J_0(\frac{u_{m,n}}{R}r)\cos(m\theta)]^2rdrd\theta} \tag{22}$$

$$B_{m,n} = \frac{1}{c\sqrt{\lambda_{m,n}}}\frac{\int_0^{2\pi}\int_0^R f(r)J_0(\frac{u_{m,n}}{R}r)\sin(m\theta)rdrd\theta}{\int_0^{2\pi}\int_0^R[J_0(\frac{u_{m,n}}{R}r)\sin(m\theta)]^2rdrd\theta} \tag{23}$$

3.2 Wave Equation with Damping

The above solution represents a non-physical situation however because the vibrations continue forever; the oscillations in time do not decay in magnitude. If we wanted to instead represent a damped oscillation in time, we can instead analyze the following equation[4]

$$\frac{\partial^2 z}{\partial t^2} = c^2\nabla^2 z - \alpha\frac{\partial z}{\partial t}, \quad \alpha > 0$$

Once again using separation of variables we obtain the two following differential equations

$$\nabla^2\phi + \lambda\phi = 0$$

$$\frac{d^2h}{dt^2} + \alpha\frac{dh}{dt} + \lambda c^2 h(t) = 0$$

The solution in space is the same both radially and angularly. However the product solution in time is now a damped ordinary differential equation. There are 3 main cases to consider when finding the solution to this equation

- Case 1: $\alpha > 2c\sqrt{\lambda}$

  For smaller modes, where λ has not grown too large in comparison to α, solutions will take the form of

$$h(t) = e^{\frac{-\alpha+\sqrt{\alpha^2-4\lambda c^2}}{2}t} + e^{\frac{-\alpha-\sqrt{\alpha^2-4\lambda c^2}}{2}t}$$

- Case 2: $\alpha = 2c\sqrt{\lambda}$ If there are any nodes where the frequency and α are balanced, the product solution will take the form of

$$h(t) = e^{-\alpha t/2} + te^{-\alpha t/2}$$

- Case 3: $\alpha < 2c\sqrt{\lambda}$ For larger nodes, where λ has grown past the magnitude of α, the solutions take the form of exponentially decaying oscillations

$$h(t) = e^{-\alpha t/2}\left[\cos\left(\alpha^2 - 4\lambda c^2\right)t + \sin\left(\alpha^2 - 4\lambda c^2\right)t\right]$$

In all cases, despite variation in the specific behavior in time, the solutions are characterized by an exponential decay in time, meaning the solution tends to zero. This matches what is expected from the behavior of a drum.

The infinite family of solutions describing individual modes of vibration is then given by

$$z_{m,n}(r,\theta,t) = J_m\left(\sqrt{\lambda_{m,n}}r\right) \cdot \begin{cases}\cos\left(\sqrt{\mu_m}\theta\right)\\ \sin\left(\sqrt{\mu_m}\theta\right)\end{cases} \cdot \begin{cases}e^{\frac{-\alpha+\sqrt{\alpha^2-4\lambda c^2}}{2}t}\\ e^{\frac{-\alpha-\sqrt{\alpha^2-4\lambda c^2}}{2}t}\end{cases} \tag{24}$$

.

for $\alpha > 2c\sqrt{\lambda}$

$$z_{m,n}(r,\theta,t) = J_m\left(\sqrt{\lambda_{m,n}}r\right) \cdot \begin{cases}\cos\left(\sqrt{\mu_m}\theta\right)\\ \sin\left(\sqrt{\mu_m}\theta\right)\end{cases} \cdot \begin{cases}e^{-\alpha t/2}\\ te^{-\alpha t/2}\end{cases} \tag{25}$$

.

for $\alpha = 2c\sqrt{\lambda}$

$$z_{m,n}(r,\theta,t) = J_m\left(\sqrt{\lambda_{m,n}}r\right) \cdot \begin{cases}\cos\left(\sqrt{\mu_m}\theta\right)\\ \sin\left(\sqrt{\mu_m}\theta\right)\end{cases} \cdot \begin{cases}e^{-\alpha t/2}\cos\left(\alpha^2 - 4\lambda c^2\right)t\\ e^{-\alpha t/2}\sin\left(\alpha^2 - 4\lambda c^2\right)t\end{cases} \tag{26}$$

.

for $\alpha < 2c\sqrt{\lambda}$

Because the damped equation did not change the eigenvalue problem for spatial coordinates, the governing shape of the waves are the same as pictured above, but decrease in magnitude until coming to rest at equilibrium over time

3.3 Empirical Results

Having developed our models to describe the vibrations of the drum head, we can now apply them to predict the motion of specific drums. Most drum heads are made out of a material called Polyethylene Terephthalate, which has an experimental density of 1.38 g/cm^3. Most drums are typically tuned with a tension force of about 16 N/cm. We will therefore assume that $c^2 \approx 11.594$. The drum we will compare our model with is a standard snare drum with a radius of 7 inches (15.24 cm).

We began by recording audio from hitting the snare drum at various different locations: the direct center, halfway between the center and the frame, and right along the frame. For each location, we created a spectrogram of the recording to determine which frequencies were the most pronounced. These results can be seen in figures 5, 6, and 7; the waveform of the recording is plotted followed by its spectrogram underneath. The x-axis of both the waveform and the spectrogram measures the time elapsed in seconds. The y-axis of the waveform is the relative volume, while the y-axis of the spectrogram is the frequencies measured in Hz. Darker colors on the spectrogram indicate higher volume frequencies.

The waveforms and spectrograms were created using Mathematica, first by importing the recordings as *Audio* objects, and then using the *AudioPlot* and *Spectrogram* commands on those objects.

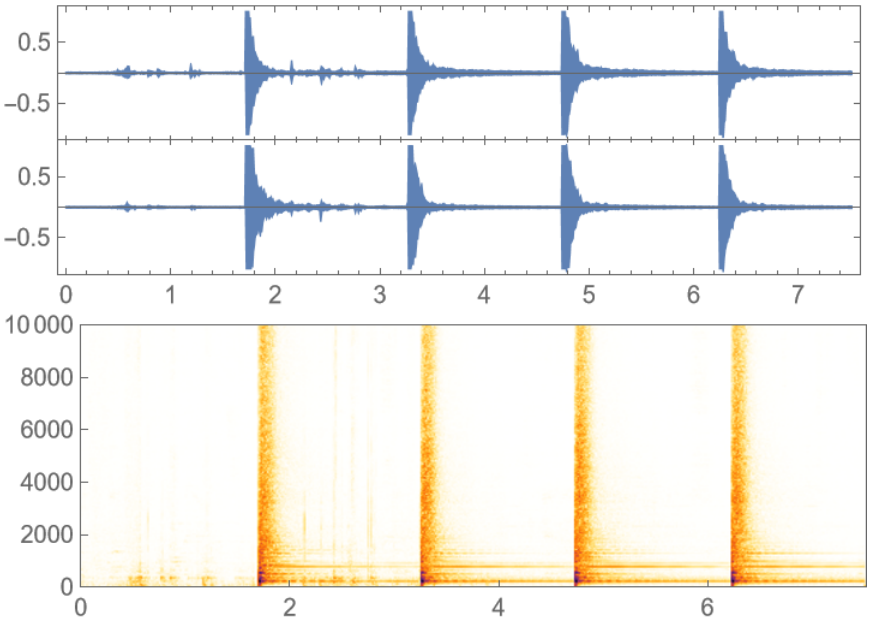

Figure 5: Waveform and Spectrogram from hitting the snare drum in its direct center

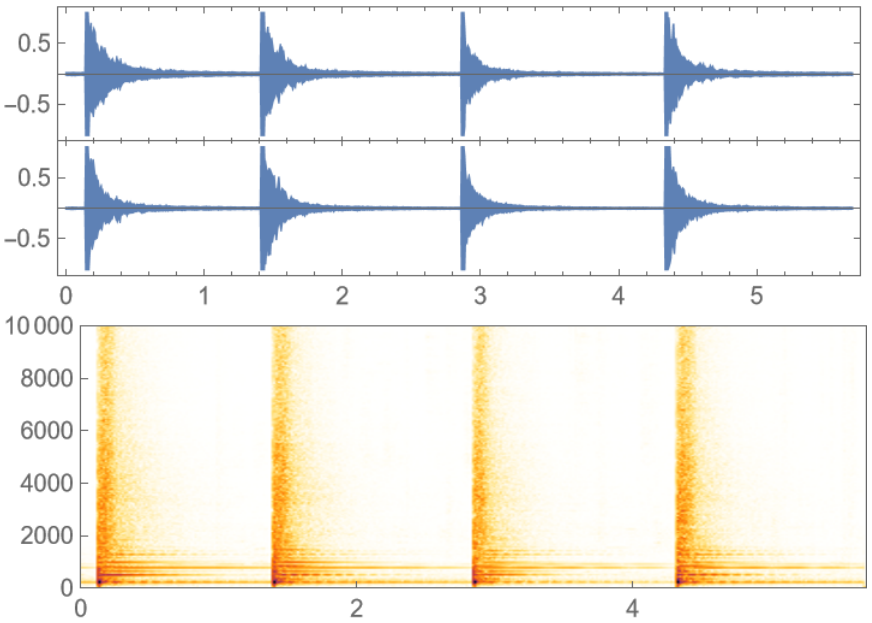

Figure 6: Waveform and Spectrogram from hitting the snare drum near its center

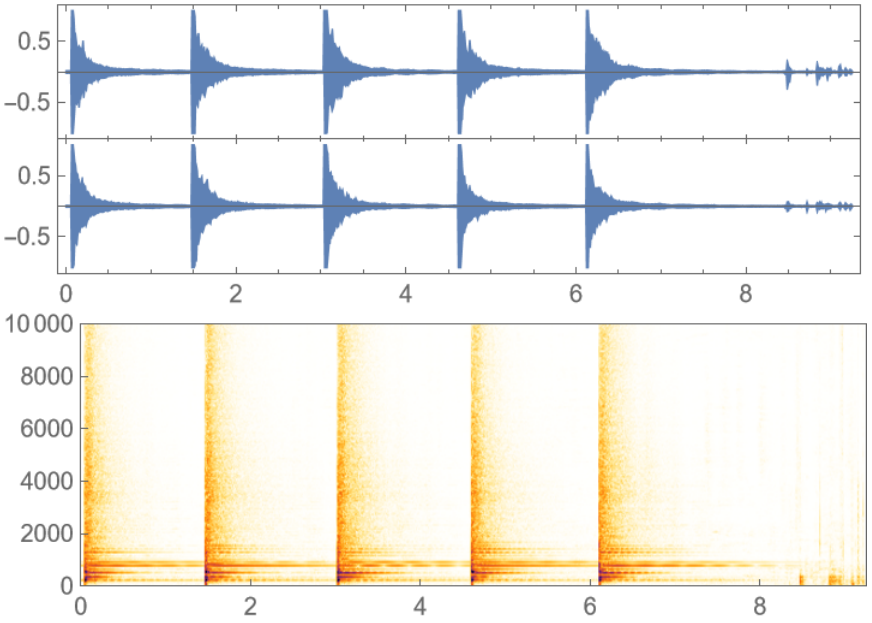

Figure 7: Waveform and Spectrogram from hitting the floor tom halfway between its center and the frame

From the figures, we see that most modes with frequencies about 2000 Hz de-

cayed to zero within about half a second; a few particular modes below 2000 Hz continued to ring out up until the next drum strike. When striking the center of the snare drum, the lower sub 2000 Hz frequencies were more intense and lasted longer; when striking halfway between the center and the frame, the higher sub 2000 Hz frequencies were more intense and persisted longer.

4 Conclusions

From the data shown above, it can be clearly seen that striking the drum in the center of the head produced much lower and more spaced out frequencies. As explained earlier, when the initial conditions are independent of θ, the solution becomes greatly simplified as the only modes included are those dependent on the Bessel function of the 0th order. Because the solution becomes only a single dimensional infinite sum, many less modes of are included. On the other hand, when the drum is struck off-center, for every mode (for smaller values of λ_{mn}) there is a corresponding infinite sum for every order of the Bessel function. This results in many more variations of frequency, creating what musicians refer to as a "fuller sound". The lack of symmetry with respect to angle allows for many more modes of vibration that vary in more than just radius. This is an important conclusion that helps to explain why musicians do not prefer to hit drums in the exact center of their head.

4.1 Further development

One of the challenges of these models is how to best represent the initial conditions. Assumptions could be made that a players hand has a constant velocity when it is actually striking the drum, which would allow for the initial derivative in time to be constant for each location on the drum head. However, representing that with a function in order to actually complete analysis of the full solution with coefficients proved to be very challenging and outside the scope of this project. Were these models to be further improved, much more analysis could be done on the initial conditions that allowed for situation-specific analysis instead of more general understandings of the modes.

Despite the lack of specific initial conditions, the actual frequency of the individual drum modes is entirely independent of the way that the drum is hit. Instead, the frequency is only dependent on the tension force of the drum (how it is tuned) and the density of the drum head material, both of which make intuitive sense. Striking the drum with different speeds or in different conditions would still create a different sound, but it would instead affect the resulting amplitude of the waves (the dynamic of the sound) and the way that the overlapping frequencies balance with each other (the timbre of the sound). As such, the frequency-specific analysis of the drum vibrations would be greatly improved by accurate measurements of these two properties of the drum. Unfortunately there is no reliable way to measure for these things.

Though the implementation of the damping term in the equation greatly improved the accuracy of the model being used, the constant α had to be arbitrarily chosen because no reliable way of measuring all of the external influences could be derived in such a format. Deriving and analyzing these conditions in a way that does not assume constant external influences would greatly improve these models and the resulting frequencies they represent.

References

[1] R. Haberman. *Applied Partial Differential Equations: With Fourier Series and Boundary Value Problems*. Featured Titles for Partial Differential Equations. Pearson, 2013. ISBN: 9780321797056. URL: https://books.google.com/books?id=hGNwLgEACAAJ.

[2] Jr. Irwin James H. "Drum sound synthesis by computer simulation of the wave equation". English. Copyright - Database copyright ProQuest LLC; ProQuest does not claim copyright in the individual underlying works; Last updated - 2023-02-21. PhD thesis. 1997, p. 132. ISBN: 978-0-591-63521-8. URL: https://colorado.idm.oclc.org/login?url=https://www.proquest.com/dissertations-theses/drum-sound-synthesis-computer-simulation-wave/docview/304353087/se-2.

[3] Richard K. Jones. *The Well-Tempered Timpani: In Search of the Missing Fundamental*. 2011. URL: https://wtt.pauken.org/.

[4] Marc Nualart. *Distributional Solutions of the Damped Wave Equation*. 2020. arXiv: 2002.04249 [math.AP].